Jan David Ytrehus[1]
SINTEF,
Trondheim 7345, Norway
e-mail: jandavid.ytrehus@sintef.no

Bjørnar Lund
SINTEF,
Trondheim 7345, Norway
e-mail: Bjornar.Lund@sintef.no

Ali Taghipour
SINTEF,
Trondheim 7345, Norway
e-mail: ali.taghipour@sintef.no

Luca Carazza
Aker BP,
Stavanger 4020, Norway
e-mail: luca.carazza@akerbp.com

Knud Richard Gyland
Schlumberger, MI-SWACO,
Stavanger 4019, Norway
e-mail: richie@start.no

Arild Saasen
Department of Energy and Petroleum Engineering,
University of Stavanger,
Stavanger 4036, Norway
e-mail: arild.saasen@uis.no

Oil-Based Drilling Fluid's Cuttings Bed Removal Properties for Deviated Wellbores

Results from cuttings transport tests in the laboratory using different field-applied oil-based drilling fluids with similar weight and varying viscosities are presented in this paper. The fluids are designed for highly deviated wells, and the cuttings transport performance at relevant wellbore inclinations was investigated. The experiments have been performed in a flow loop that consists of a 10-m-long test section with 50.4 mm (2″) diameter freely rotating steel drill string inside a 100-mm (≈4″) diameter wellbore made of cement. Sand particles were injected while circulating the drilling fluid through the test section. Experiments were performed at three wellbore inclinations: 48, 60, and 90 deg from vertical. The applied flow loop dimensions are designed so that the results are scalable to field applications; especially for the 12 ¼″and 8 ½″ sections. The selected setup provides correct shear rate ranges and similar Reynolds numbers to the field application when the same fluids are applied. Results show that hole cleaning abilities of the tested fluids vary significantly with well angle, drill string rotation, and flowrate. Results support field experience showing that low viscous fluids are more efficient than viscous fluids at higher flowrates and low drill string rotation. As well as per field experience, more viscous fluids are efficient in combination with high drill string rotation rates. The results show the effect of cuttings transport efficiency as a function of hydraulic frictional pressure drop, demonstrating methods to achieve a more optimal hydraulic design in the tested conditions. The key findings have direct relevance to drilling operations. [DOI: 10.1115/1.4050385]

Keywords: petroleum engineering, petroleum wells-drilling/production/construction

Introduction

A drilling fluid for drilling deviated wellbores must provide adequate hole cleaning efficiency for well angles relevant to the well construction operation. For well inclinations near vertical, practical experience and laboratory studies have shown that hole cleaning is straightforward. In deviated wellbores, hole cleaning is more challenging. Cuttings beds can be formed both during drilling and at the stop in circulation, and these beds should be removed through proper fluid choice and operational practices.

Deviated well sections are common. In mature areas like the North Sea region, practically all producers or injector wells will have highly deviated sections. These wells must be drilled and completed optimally with respect to drilling time, cost, risk, and functionality. Most cuttings transport and hydraulic models are developed based on tests with model fluids and often in small diameter test sections. Both the laboratory fluids and the size of the experimental equipment are a challenge in itself [1]. Hole cleaning and hydraulic behavior with field fluids are different from the achieved results obtained with most model fluids. Hence, there is a need for studies in controlled laboratory environments with various used or fresh field fluids tested in sufficiently large experimental flow loops to avoid scaling problems, in order to improve engineering models and practices.

Models for hydraulic friction or equivalent circulating density (ECD) are needed to plan the drilling operation. ECD is defined as the drilling fluid density plus the frictional pressure loss divided by gravity and vertical depth in consistent units. These models rely on empirical data to close the equation sets. Controlled experiments providing results used for this work are normally from small-scale laboratories. For practical reasons, such experiments are performed with fairly simple water-based fluids. This means that many hydraulic models are developed based on simplified fluids systems in downscaled setups, which may often produce inadequate results, as shown by Saasen [1]. Cuttings transport efficiency of oil-based fluids can differ from that of water-based fluids [2] even if the fluids appear to have similar flow curves and fluid characteristics according to API. Possible explanations include different colloidal effects [3] and the presence of normal stress differences in water-based drilling fluids [4].

In two comprehensive review articles, Li and Luft [5,6] summarized experimental studies and theoretical analyses of hole cleaning. Experiments have also shown that hole cleaning can be different in gauge open hole and inside casing [7]. Numerical simulations have also been used to evaluate hole cleaning [8,9]. Using such model approaches would provide similar results for oil-based and water-based fluids of similar viscosities and densities. From Sayindla et al. [2], it is known that differences would still appear. To support previous simulators and motivate improved numerical models, experiments in controlled conditions with various types of oil-based fluids can be of significant value. The purpose of the present article is to present experimental results and explain several flow phenomena occurring during practical drilling operations in order to optimize drilling operations. To perform this enterprise, it is necessary to show experimental hole cleaning results from tests with selected oil-based drilling fluids with different properties. These drilling fluids were all field fluids from operations on the Norwegian Continental Shelf.

Experimental Procedures

The experiments are conducted in the flow loop pictured in Fig. 1 and shown schematically in Fig. 2. This experimental facility is constructed as an annulus with a free whirling motion of the fully eccentric drill string during the drill string rotation, as illustrated

[1]Corresponding author.

Contributed by the Petroleum Division of ASME for publication in the JOURNAL OF ENERGY RESOURCES TECHNOLOGY. Manuscript received October 28, 2020; final manuscript received February 22, 2021; published online March 18, 2021. Assoc. Editor: Ray (Zhenhua) Rui.

Fig. 1 Picture of the flow loop test section in a horizontal position

in Fig. 3. The motion of the drill string was kinematically constrained only by the interior wall of the wellbore and of a universal joint which was at the downstream flow end of the test section. Thus, the whirling motion was not controlled. Although the lateral motion was not monitored directly, experimental conditions and torque measurements indicate that the motion was not a fully developed whirl, but rather an oscillatory motion about the lowest point of the wellbore. The test section is constructed such that it can tilt between angles from 90 deg (horizontal) to 48 deg. The annular dimensions of the flow loop are selected near the minimum of what may be considered relevant to compare the results with field experience. The fluid circulation system is constructed so that field fluids, both oil-based and water-based, can be used. The closed circulation system includes a particle handling system allowing dry cuttings to be injected from a feeder tank using a screw pump for granular solids and then carried once through the flow loop with the circulating drilling fluid and removed in the separation unit. The feed rate was controlled by the frequency of the pump, after an initial calibration to ensure the correct mass rate. The presented experiments are conducted both without particles and with quartz sand particles in the size range from 0.9 mm to 1.6 mm. The sand was purchased from Dansand A/S.

The experimental setup, shown schematically in Fig. 2, consists of the following main components:

(1) drilling fluid storage tank;
(2) sand injector unit;
(3) liquid slurry pump;
(4) density and flowmeter;
(5) test section with pressure and differential pressure transducers;
(6) sand separator; and
(7) sand reception system and fluid return to the storage tank.

The 10-m-long test section is built with an outer support pipe, into which a continuous series of hollow cement inserts are placed to represent an open wellbore wall.

Hollow cylindrical sections of cement, all with outer annular diameter, $D_o = 100$ mm (4″), were applied. The drill string is represented by a steel rod of $D_i = 50.4$ mm (2″) diameter inside the wellbore and defining the inner diameter of the annular test section. For additional information about the experimental equipment, please consult Ytrehus et al. [10]. Saasen [1] concluded that "even though laboratory experiments are necessary to improve the understanding of well flow phenomena, is not straightforward to use experimental results directly to create correlations. The complexity of the geometry and fluid properties includes far too many dimensionless quantities that need to be within the same range to be valid". The dimensions of the test section are of the same order of magnitude as those used for drilling operations in 8 ½″ section and 12 ¼″ section in the present case, making it possible to simulate real conditions in the laboratory.

The focus of the experiments was to obtain steady-state conditions while circulating drilling fluid without or with injected cuttings. Steady-state was assumed to have been obtained when the tank weight reading had reached a constant level after having changed a process parameter (flowrate, cuttings injection rate, or string rotation speed).

Fluid and Viscosity Parameters

Three field-applied oil-based drilling fluids were used in the experiments, labelled OBM A (low viscosity), OBM B (medium viscosity), and OBM C (high viscosity). All the fluids are typically used for ERDwells, and OBM A is constructed with very low viscosity to minimize the dynamic pressure drop and is referred to as a low ECD fluid. OBM B is considered a more standard oil-based drilling fluid. OBM C is categorized as a "flat viscosity" fluid, meaning that there is little variance in the viscosity profile over a large temperature span. Their viscous properties were measured using an Anton Paar 102 rheometer. Flow curve data are plotted in Fig. 4 for the relevant shear rate range in annular flow.

All fluids were constructed using non-aromatic base oils. The fluids mainly consist of conventional OBM components for North Sea applications. In OBM A, a micronized barite is used as a weighting material. Further information on this fluid can be found in the study by Ytrehus et al. [7,10]. For OBM C, a fine-grained barite is used as a weighting material.

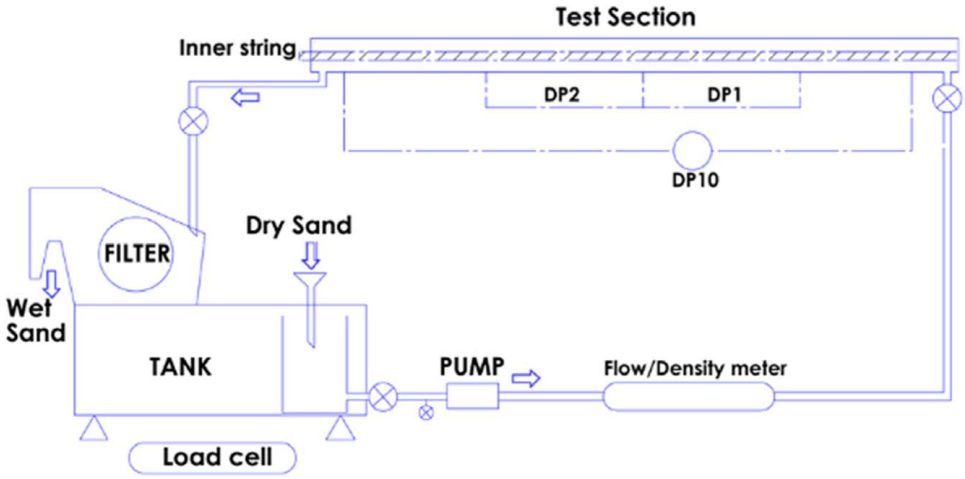

Fig. 2 Sketch of the flow loop

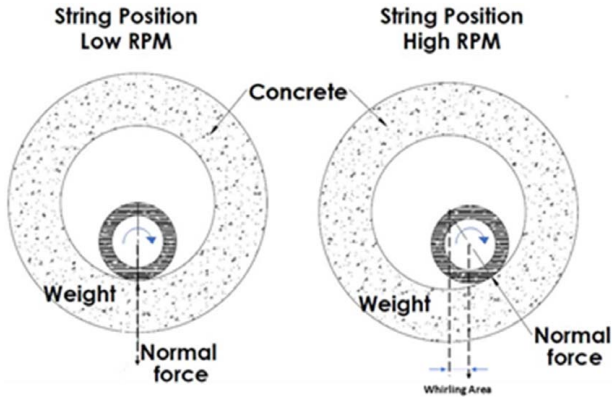

Fig. 3 Sketch of drill string rotation and whirl during the experiments

During the period of flow loop experiments, the viscous properties were measured frequently to ensure proper control of the relevant fluid properties. The drilling fluid viscosities are described through the Herschel–Bulkley model. The viscous parameters are presented in Table 1. The representation of the Herschel–Bulkley model from Saasen and Ytrehus [11,12] follows Eq. (1). The shear stress is given as

$$\tau = \tau_y + \tau_s \left(\frac{\dot{\gamma}}{\dot{\gamma}_s}\right)^n \tag{1}$$

where the surplus stress, $\tau_s = \tau - \tau_y$ is measured at a representative shear rate of $\dot{\gamma}_s$. This surplus stress is selected at 198 s^{-1}, ($\dot{\gamma}_s = 198$ s^{-1}), and the flow behavior index n is calculated by matching the shear stress at 61 s^{-1}. As seen in Fig. 4, these parameters provide good matches with the flow curves within the relevant shear rate range for all three fluids.

The traditional consistency index k can be expressed in terms of the surplus stress τ_s and the representative shear rate $\dot{\gamma}_s$ as

$$k = \tau_s \left(\frac{1}{\dot{\gamma}_s}\right)^n \tag{2}$$

Table 1 Summary of relevant fluid parameters at 25 °C

Fluid	τ_y (Pa)	τ_s (Pa)	τ_{198} (Pa)	n	K (Pa · s^n)	ρ (kg/m^3)
A	0.196	*3.93*	*4.13*	0.88	0.0374	1430
B	1.29	8.71	10.0	0.78	0.1408	1440
C	1.8	10.6	12.3	0.82	0.1387	1490

Note: Herschel–Bulkley variables are calculated from the flow curves shown in Fig. 4 at 198 s^{-1}. n is calculated at 61 s^{-1} for the dimensionless model.

In the calculation of the fluid parameters, the yield stress τ_y was determined in accordance with Power and Zamora [13] by $\tau_y = 2\tau_3 - \tau_6$, where τ_3 and τ_6 represent the 3 and 6 rpm readings in the Fann viscometer data.

Circulation Pressure Drop

To be able to evaluate the hole cleaning capabilities, it is necessary to understand the frictional pressure losses resulting from pumping the actual fluids.

Frictional Pressure Loss Model. The calculations are performed using a model for annular frictional pressure loss with Herschel–Bulkley fluids as described by Founargiotakis et al. [14]. The model uses the slot approximation for laminar flow in a concentric annulus. A correction was applied for eccentricity in laminar flow using a correlation which was published by Haciislamoglu and Langlinais [15]. The eccentricity correction is expressed in terms of a correlation:

$$R(\varepsilon, \kappa, n) = \frac{\left(\frac{dp}{dx}\right)_{ecc}}{\left(\frac{dp}{dx}\right)_{conc}} \tag{3}$$

between pressure gradient in eccentric and concentric annuli, respectively, where ε is eccentricity and κ is the ratio of D_i over D_o.

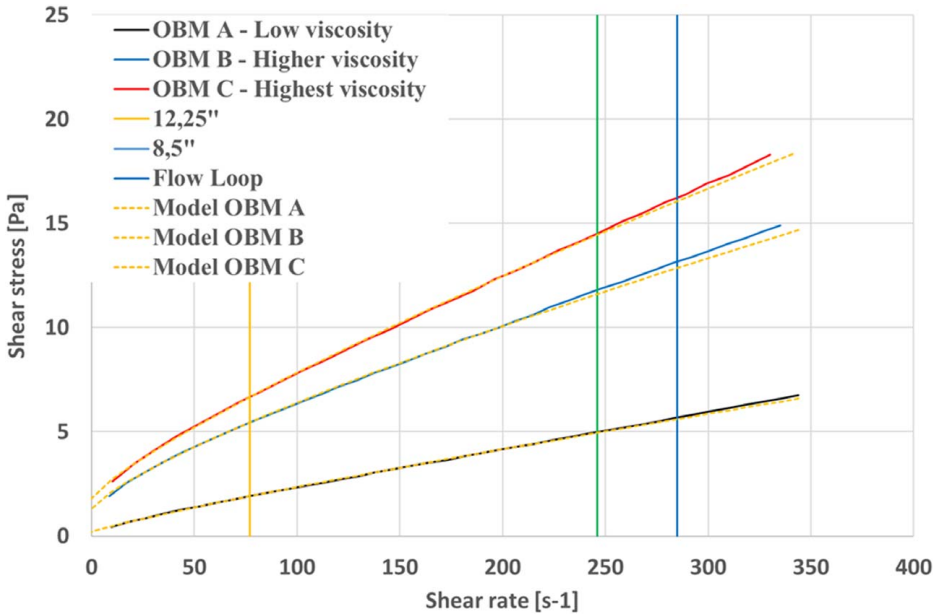

Fig. 4 Plot of flow curve for the applied OBMS in relevant shear rate range. Maximum shear rates in annular flow for 8 ½″ and 12 ¼″ sections with 5 ½″ drill pipe are shown based on operational pump rates. The shear rate limit in the flow loop in the applied tests is also shown. Both measurements and model data are shown.

For turbulent flow the correlation developed by Haciislamoglu and Cartalos [16] for a power-law fluid was used. This fluid was adapted to a yield stress fluid following Kelessidis et al. [17], using the flow behavior index n in the correlation. Using the generalized flow behavior index n' in this correlation may give significantly different results. For turbulent flow the model uses a friction factor correlation

$$\frac{1}{\sqrt{f_{turb}}} = \frac{4\log_{10}[\mathrm{Re}_{MRa} f_{turb}^{1-n'/2}]}{(n')^{0.75}} - \frac{0.395}{(n')^{1.2}} \tag{4}$$

The Fanning definition of friction factor is:

$$f = \frac{\tau_w}{\rho U^2/2} \tag{5}$$

Re_{MRa} is the generalized (Metzner-Reed) Reynolds number defined by

$$\mathrm{Re}_{MRa} = \frac{\rho U D_h}{\mu_e} \tag{6}$$

where D_h is the hydraulic diameter

$$D_h = D_o - D_i \tag{7}$$

and the effective viscosity is defined as

$$\mu_e = \frac{\tau_w}{\dot{\gamma}_{Nw}} \tag{8}$$

where

$$\dot{\gamma}_{Nw} = \frac{12U}{D_o - D_i} \tag{9}$$

is the wall shear rate of a Newtonian fluid at the same average flow velocity U (note a misprint in Founargiotakis et al. [14]). Note that this definition of Reynold's number gives the same familiar friction factor law

$$f_{lam} = \frac{24}{\mathrm{Re}} \tag{10}$$

for laminar flow as in the Newtonian case.

The friction factor correlation used for calculating turbulent flow assumes smooth pipes. Thus, for rough pipes, the prediction may underestimate the frictional pressure drop in the turbulent flow regime.

Verification of Pressure Drop Model. The pressure loss calculations must be verified by experiments. Also, a baseline for the hole cleaning experiments must be formed. As seen in Fig. 5, the model reproduces the laminar pressure loss data well for the most viscous OBM C and fairly well for OBM B, although with some overprediction. For the least viscous fluid A, the match is less satisfactory. However, there is only one data point, at 0.5 m/s, which is in a truly laminar regime and where the model fits well.

In the rest of this section, OBM A is discussed, which is the only of these three fluids showing non-laminar behavior. At 0.7 m/s, the Reynolds number is already well above 2000, and transitional flow effects may have increased the pressure gradient. Haciislamoglu and Cartalos [16] found that the pressure loss reduction due to eccentricity is smaller in the transitional region than both in the laminar and in the turbulent regions. This effect has not been modeled here, which may account for the discrepancy in this region. However, the discrepancy between model and experiments in the turbulent region remains to be explained.

The model gives a fairly abrupt transition to turbulence with a discontinuity, at around 0.75 m/s for fluid A. The experimental data show a more gradual transition to turbulence. The softer transition can be attributed both to the eccentricity and to the non-Newtonian behavior.

The model predicts a transitional region between laminar and turbulent flow around 0.75 m/s, corresponding to a Reynolds number of about 2300. This seems to be consistent with the experimental data, although it is not possible to identify the start and end of the transitional region due to the limited number of data points.

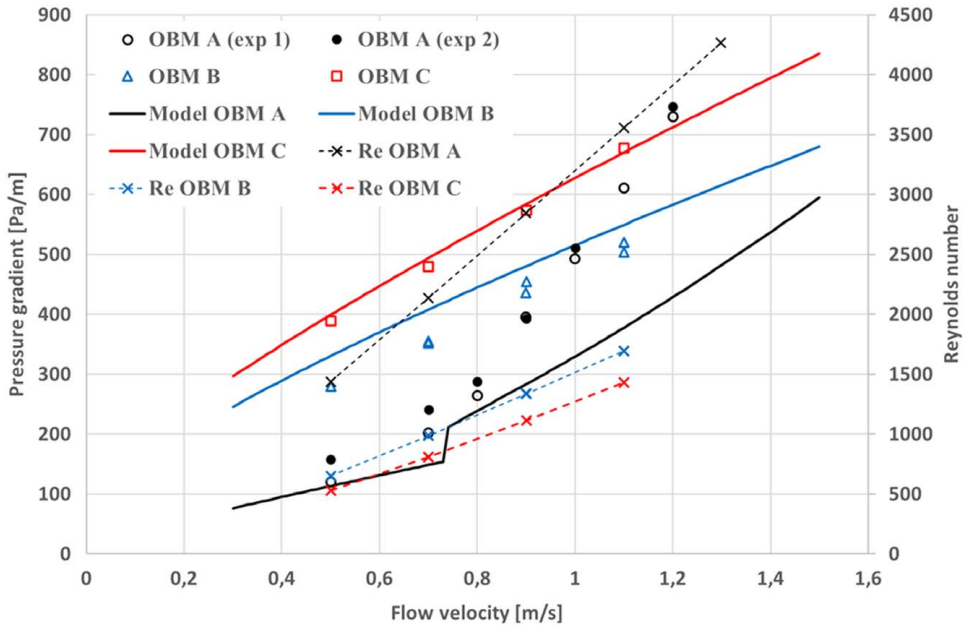

Fig. 5 Plot of measured and calculated pressure gradient as a function of flow velocity for three OBMS in the horizontal, eccentric annulus in absence of rotation and without cuttings: OBM A (low viscosity), OBM B (medium viscosity), and OBM C (high viscosity). Reynolds numbers for the fluids are also plotted on the secondary *Y*-axis.

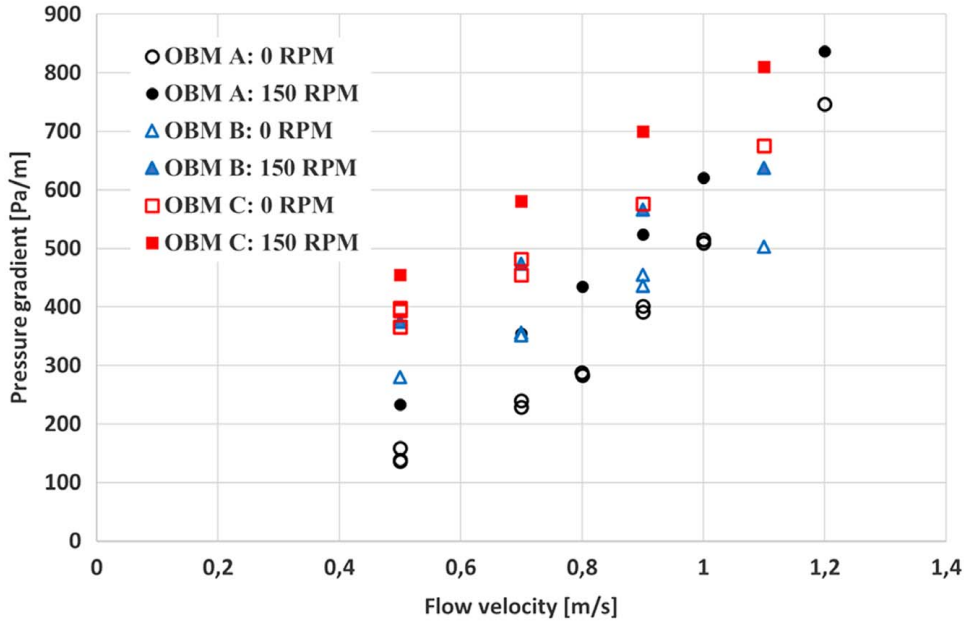

Fig. 6 Plot of measured pressure drop at different flow velocities for the three OBMS in horizontal eccentric annulus when no cuttings are present: OBM A (low viscosity), OBM B (medium viscosity), and OBM C (high viscosity). The string rotations presented are 0 and 150 rpm.

The pressure drops increase as expected when string rotation is added for all applied fluids. This is plotted in Fig. 6. It is observed that OBM A has a steeper pressure drop increase than OBM B and OBM C for velocities above the laminar region both with and without rotation.

Hole Cleaning Experiments

In evaluating the hole cleaning ability of the fluids, the effects of pump rate, drill string rotation and inclination are considered. The hole cleaning ability is quantified in terms of an equivalent relative cuttings bed height, which is the bed height (normal to wellbore axis, divided by wellbore diameter), which would be formed if all cuttings particles were sedimented on the low side of the annulus (assuming a close packing porosity). The actual bed height will be somewhat smaller since some of the particles are in suspension during transport, but the contribution of the suspended particles is relatively small.

The bed height was determined indirectly from the measurement of the tank weight, using mass balance, and assuming a representative porosity.

Entrance and exit effects will of course affect the results to some extent. These effects are not quantified. However, entrance length for bed creation is anticipated to be relatively small and should not affect the measurements. This is illustrated in Fig. 7. The figure shows the tank weight versus time for a sample experiment during the buildup of a bed, starting from the situation with no cuttings in the test section. As the cuttings are transferred from the tank to the test section, the weight of the tank decreases. Any accumulation of cuttings in the test section, including in the entrance, will show up on the tank weight, due to mass balance. A linear decrease indicates a bed front moving with constant velocity through the test section. A sharp transition from a constant tank value to a linear

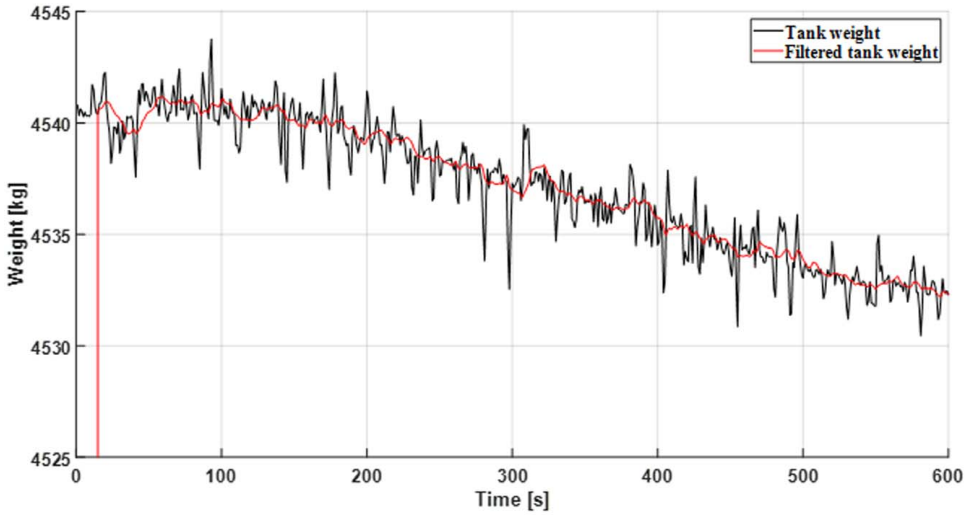

Fig. 7 Plot of weight cell responses (actual and filtered) as a function of test time during a typical bed buildup situation

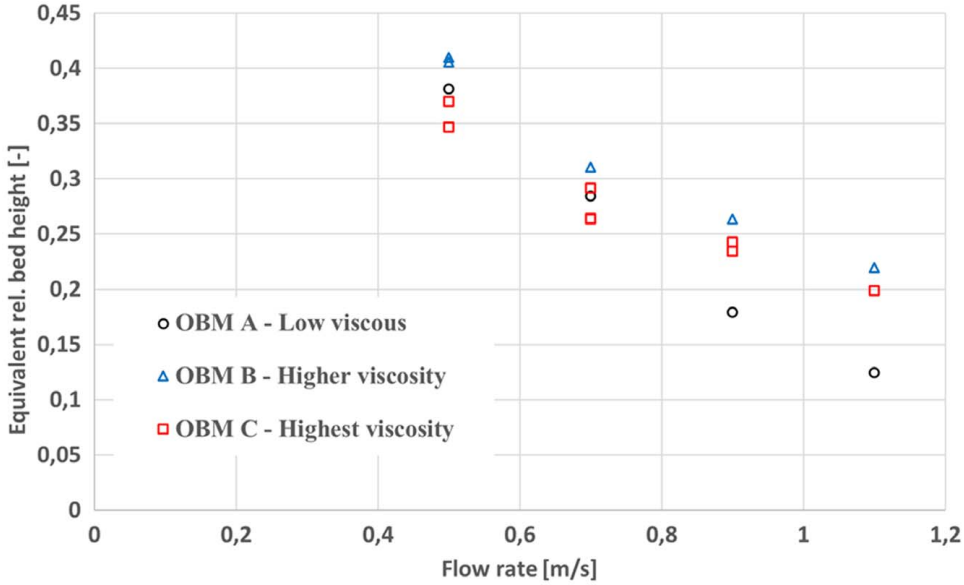

Fig. 8 Sandbed height as a function of superficial velocity in horizontal, eccentric annulus without drill string rotation. Sand injection rate is 43 g/s.

decrease indicates that the entrance effects are small. Since the annulus is straight and of uniform cross section, the accumulation of cuttings in the test section is expected to be a linear process, at least in a horizontal annulus, with a bed front moving at a constant speed. Any accumulation of cuttings in the inlet section (pipes and fittings) would generally proceed at a different rate. Any significant accumulation here is therefore expected to show in the transition from the initial constant tank weight to the decreasing tank weight. Similarly, a sharp transition from the linearly decreasing tank weight to a constant tank weight indicates that exit effects are not significant.

The cuttings bed height for a case without string rotation and in the horizontal test section is plotted in Fig. 8. This plot shows that at low flow velocities the most viscous fluid, OBM C, appears to give a lower sand bed than the least viscous, OBM A. After a transition point, somewhere between 0.7 and 0.9 m/s, the low viscous OBM A provides a significantly lower sand bed than the two others. For all the applied velocities OBM B, the second most viscous fluid provides the highest sand bed and thus the poorest hole cleaning. These results imply that there is a threshold value, likely related to the transition from laminar to the non-laminar regime as indicated in Fig. 5. The cuttings transport performance of the low viscous OBM A is significantly dependent on which side of this transition flowrate the flow conditions are. Since the more viscous fluids appear to stay within the laminar flow regime for all the applied flowrates, similar effects are not observed for these.

In Fig. 9, the sand bed height is plotted as a function of the pressure gradient. The ordinate, the sand bed height measurements, is the same as in Fig. 8, but the abscissa is the measured frictional pressure loss obtained when pumping with the flowrates used in

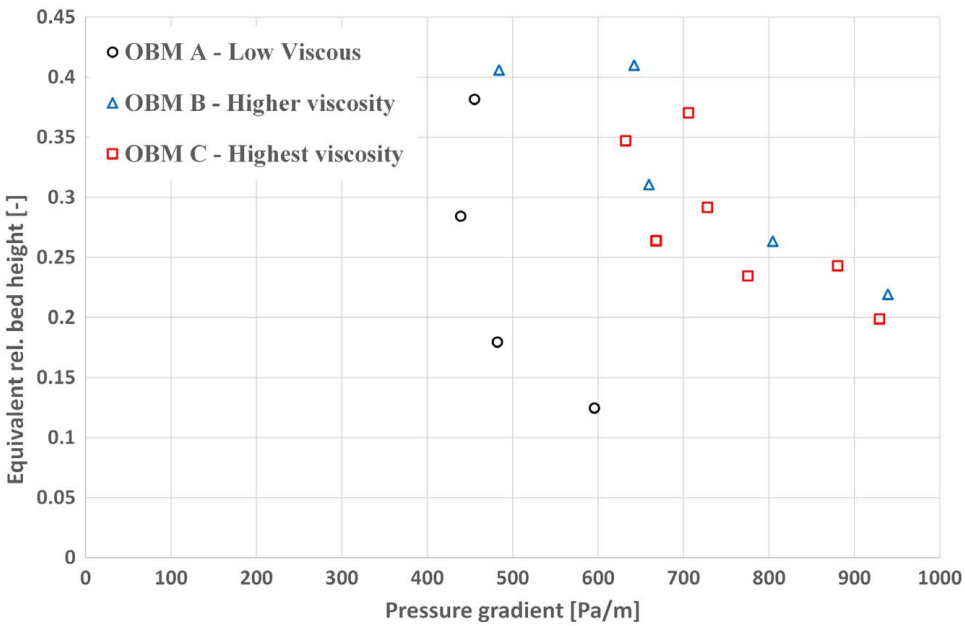

Fig. 9 Sandbed height as a function of pressure drop (ECD) in the absence of drill string rotation at horizontal conditions. Sand injection rate is 43 g/s.

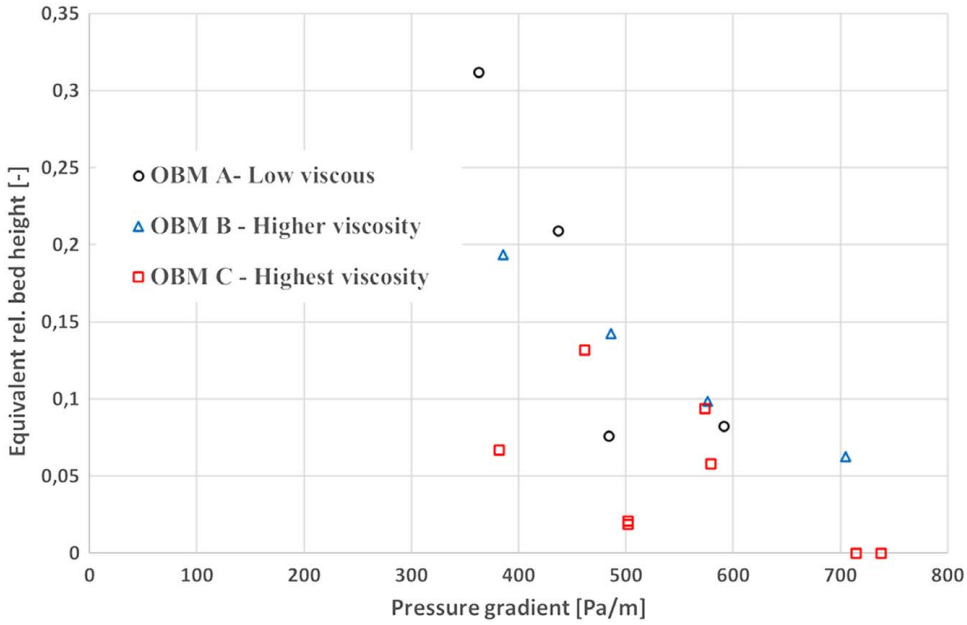

Fig. 10 Sandbed height as a function of pressure drop (ECD) in the case with 50 rpm drill string rotation at horizontal conditions. Sand injection rate is 43 g/s.

the measurements shown in Fig. 8. The low viscous fluid, OBM A, can be considered more effective than the more viscous fluids for all tested flow velocities with respect to hole cleaning as a function of the pressure loss. In the absence of particles, the flow of the most viscous OBM, OBM C, produced the highest frictional pressure loss as was shown in Fig. 5. This higher pressure loss was not observed in the hole cleaning experiments. The flow of the most viscous fluid, OBM C, does not produce a higher pressure drop gradient than OBM B in these cases. This implies that the viscous effects on the pressure losses are compensated by a higher flow area due to better particle bed removal effects for OBM C than for OBM B. It can also be observed from the experiments with OBM A that an increase in flowrate gives only small effects on the frictional pressure drop until the flow reaches a threshold value just below 0.9 m/s. At the lower flowrates applied in the tests, the flow area changes such that the frictional pressure loss value becomes fairly constant. At higher flowrates than this threshold value, the main contribution to the frictional pressure loss is in the wide area of the annulus. An increase in frictional pressure loss will also imply an increase in the wall shear stress onto the cuttings bed and improve hole cleaning. However, this improved hole cleaning will not give a significant reduction in cuttings bed area compared to the cross-sectional flow area, as this remaining bed is placed in the narrow part with only small shear rates. Hence, this increased flowrate will not result in a sufficient increase in flow area to keep the pressure loss constant above the threshold flowrate value.

When drill string rotation is introduced, the more viscous fluids become more efficient compared to the low viscous OBM A (see Figs. 10 and 11). The cuttings transport efficiency in the presence

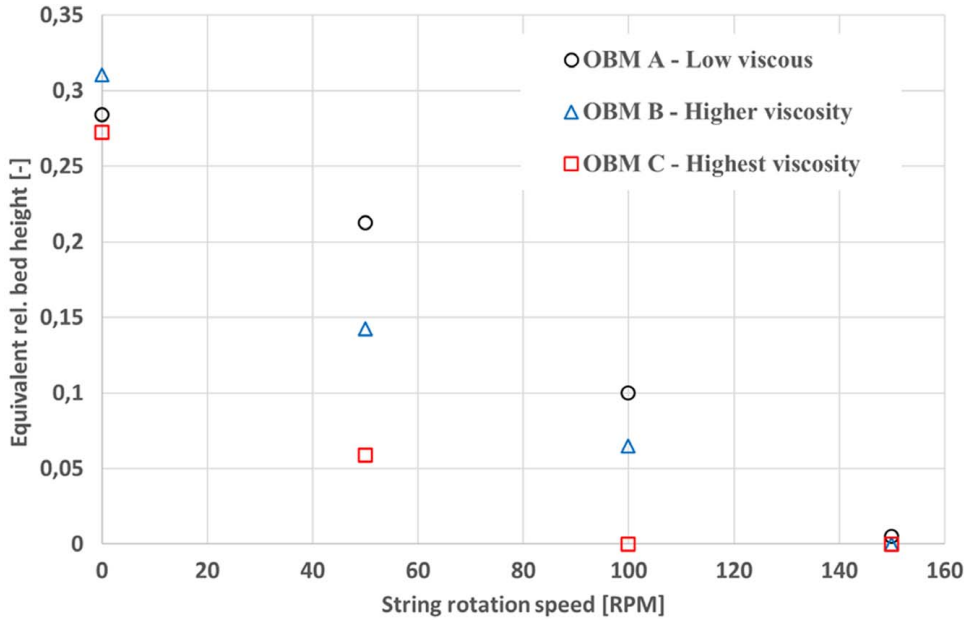

Fig. 11 Sandbed height at an annular velocity of 0.7 m/s as a function of drill string rotation. Sand injection rate is 43 g/s.

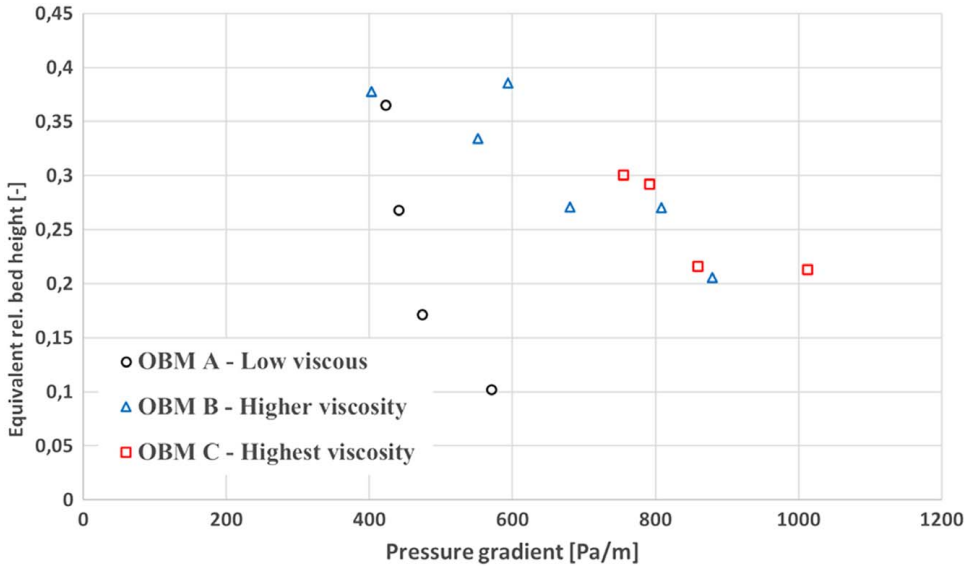

Fig. 12 Sandbed height as a function of pressure drop (ECD) in the absence of drill string rotation at 60 deg test section deviation. Sand injection rate is 43 g/s.

of drill string rotation rate of 50 rpm (Fig. 10) is better than without string rotation for all fluids and all flowrates tested. The experiment with the most viscous fluid, OBM C, produce the lowest sand bed height in almost all tested cases. This is most likely caused by a more efficient viscous coupling between the rotating drill string and the flow. The frictional pressure drops appear to be nearly similar for each flowrate for all the tested fluids at 50 rpm. In Fig. 11, it is seen that the sand bed height is reduced close to linearly from 50 rpm and up to 150 rpm until the bed is totally removed. The sand bed height for each drill string rotation above zero is correlated with the viscosity of the fluids. The results imply that when the sand bed is disturbed by the drill string rotation and the sand particles are distributed through the flowing area, a higher fluid viscosity provides better cuttings transport efficiency. This may be because of longer settling time in higher viscosity fluids than in low viscous fluids, while the erosion of a cuttings bed seems to be more efficient with low viscous fluids compared to high viscous when no external agitation is introduced. This can explain why the fluid performance efficiency in horizontal conditions shifts when drill string rotation is introduced.

The observations at an inclination of 60 deg from vertical were different from those in the horizontal annulus. This difference is observed both without drill string rotation (Fig. 12) and with drill string rotation (Fig. 13). It appears that the flow of OBM A provides an overall lower cuttings bed height than the other fluids. Similarly, a significantly lower corresponding frictional pressure drop is observed for the flow with OBM A for almost all tests at this inclination. Furthermore, there is a tendency that the flow with the most viscous fluid, OBM C, experiences a higher pressure drop than OBM B while the sand bed height appears to be close to similar for these two fluid experiments. From the experimental results, it seems like the frictional pressure drop also with sand is highly related to the viscosity of the fluids. Differences in cuttings transport efficiency between the tested fluids appear to be relatively little

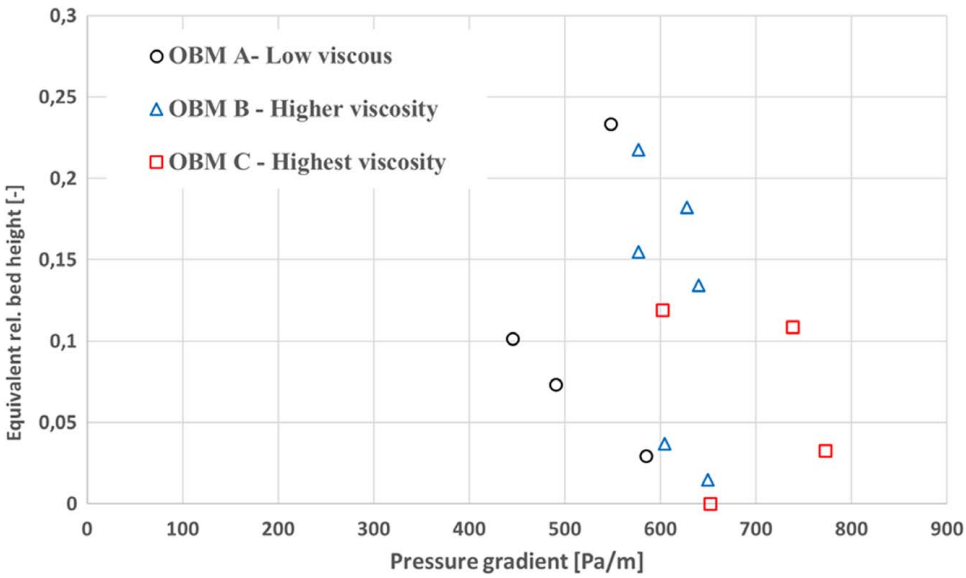

Fig. 13 Sandbed height as a function of pressure drop (ECD) in the presence of 50 rpm drill string rotation at 60 deg test section deviation. Sand injection rate is 43 g/s.

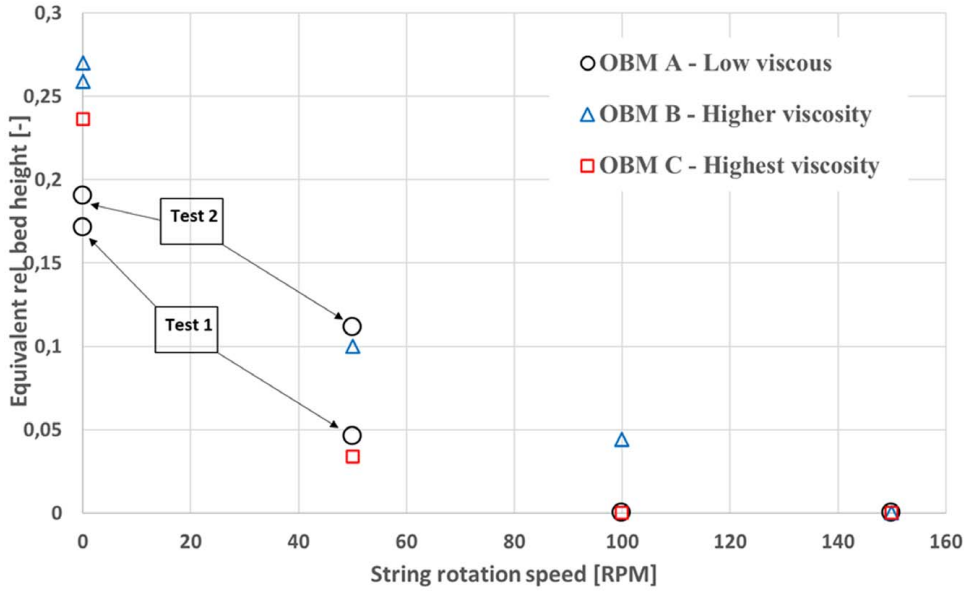

Fig. 14 Sandbed height at an annular velocity of 0.9 m/s as a function of drill string rotation. Sand injection rate is 43 g/s.

affected by string rotation at 60-deg inclination. Most likely a larger portion of the flow volume of OBMs B and C flows in the wide part of the annulus. This is expectedly a consequence of the larger degree of shear-thinning in these fluids compared to the degree of shear-thinning in OBM A. All these observations may imply that flow properties at the bed surface are more important than for instance sand suspension efficiency at the core of the fast-moving drilling fluid at this inclination.

Figures 11 and 14 show the effect of drill string rotation on sand bed height in a horizontal annulus at fluid superficial velocities of 0.7 m/s and 0.9 m/s, respectively. In Fig. 14, two tests for OBM A are shown, where Test 2 is a repetition of Test 1. Here, Test 2 is anticipated to be trusted more, as there was more noise in the Test 1 time data series. In the absence of drill string rotation, good hole cleaning performance is obtained using a thin drilling fluid at a sufficiently high pump rate. This is illustrated by comparing the results for no rotation in these two figures. At 0.7 m/s superficial velocity, the hole cleaning ability is somewhat similar. Too many particles are still left in the hole. When the superficial velocity is increased to 0.9 m/s, the hole cleaning performance of the thinnest drilling fluid is significantly improved. Also, the performance using the two other fluids is improved, but not to the same degree. Adding rotation to the drill string will generally increase pressure loss [18] but also improve hole cleaning, especially for slow viscous flow. This improvement is verified as the hole cleaning ability of the most viscous fluid (OBM C) is significantly improved, even at the lowest flowrate, by the addition of a low 50 rpm rotation rate. The degree of improvement is lowest for the thin fluid (OBM A), while the improvement for the medium viscous fluid (OBM B) is between OBM A and OBM C. At 100 rpm, the rotation rate is sufficient to clean the hole totally for the most viscous fluid at 0.7 m/s. For the use of the thinnest fluid, a higher flowrate was needed to obtain a similar result. However, the frictional pressure loss is lower while pumping the thinnest

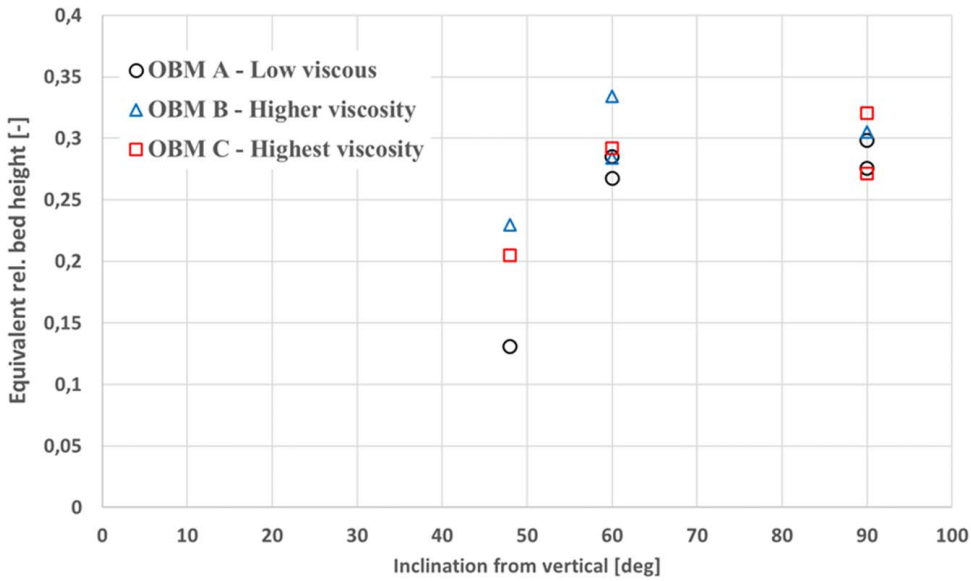

Fig. 15 Sandbed height at an annular velocity of 0.7 m/s as a function of test section deviation angle in the absence of drill string rotation. Sand injection rate is 43 g/s.

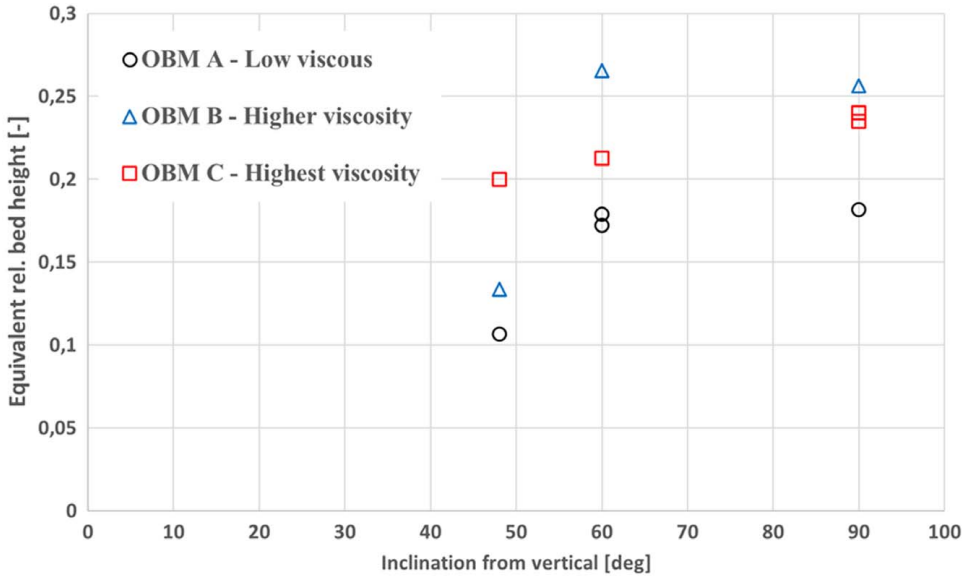

Fig. 16 Sandbed height at an annular velocity of 0.9 m/s as a function of test section deviation angle in the absence of drill string rotation. Sand injection rate is 43 g/s.

fluid at 0.9 m/s at 100 rpm rotation rate than when pumping 0.7 m/s at 100 rpm with the most viscous fluid.

As known, the well angle has a great influence on the hole cleaning abilities. In Fig. 15, it is shown the hole cleaning ability of the fluid flows in cases without drill string rotation at a superficial velocity of 0.7 m/s. For the well angles from 60 deg to 90 deg, the hole cleaning abilities of the fluids are similar. At an angle of 48 deg, without discussing the lag time of the cuttings, the hole cleaning ability is generally better. In this case, the thinnest drilling fluid provides the best hole cleaning.

When the superficial velocity is increased to 0.9 m/s, as shown in Fig. 16, flow properties become more important and the lowest viscous drilling fluid provides the best hole cleaning. This is anticipated to be due to the appearance of turbulent behavior in the widest part of the cross-sectional area.

There is a difference in the performance of the two most viscous drilling fluids at the velocity of 0.9 m/s. The most viscous fluid provides better performance as the well angle is reduced. Still, this most viscous fluid never reaches the ability of the thinnest fluid's performance for well angles larger than 48 deg. The medium viscous fluid provides the poorest hole cleaning performance at well angles of 60 deg and larger. However, at 48 deg and 0.9 m/s superficial flow velocity, OBM B provides a significantly better hole cleaning than the viscous OBM C, but not as good as the thin OBM A.

Based on the observations from Figs. 15 and 16, it is fair to say that OBM A is superior with respect to hole cleaning for all tested inclination angles when drill string rotation is absent.

Conclusions

A set of experiments has been conducted with field-applied oil-based drilling fluids. The following points have been verified for drilling fluid flow in a fully eccentric annulus:

- Annular frictional pressure losses can be predicted using the slot model for laminar well flow as long as the viscous parameters are developed to be applicable for the relevant shear rates of the well flow.
- Hole cleaning performance is better using low viscosity drilling fluids in the absence of drill string rotation.
- The efficiency of the more viscous drilling fluids is improved by the addition of drill string rotation.
- Flow of the more viscous drilling fluids produces a higher ECD. Hence, in the case of narrow ECD windows, hole cleaning can be better with low viscosity drilling fluids at high pump rates. In the presence of wide ECD windows, the use of viscous drilling fluids may provide the best hole cleaning performance in horizontal well sections.
- There is an ECD restriction constraining if low viscosity drilling fluid should be used at higher pump rates or if viscous drilling fluids should be used at low pump rates for highly deviated wells.

Acknowledgment

The authors thank Aker BP for supporting the experimental work. The authors thank Schlumberger MI-SWACO fluids for providing the fluids and technical support required for completing this work. Finally, the authors would like to thank the Research Council of Norway (Grant No. 294688) for the financial support of the publication.

Conflict of Interest

There are no conflicts of interest.

Nomenclature

f = friction factor
k = consistency index
n = flow behavior index
U = average flow velocity in the annulus
n' = generalized flow behavior index
D_h = hydraulic diameter
D_i = inner diameter of the annulus (diameter of steel rod)
D_o = outer diameter of the annulus
dp/dx = frictional pressure gradient
Re = Reynolds number
$\dot{\gamma}$ = shear rate
$\dot{\gamma}_{Nw}$ = equivalent wall shear stress in a Newtonian fluid
$\dot{\gamma}_s$ = representative shear rate
μ_e = effective viscosity
ρ = fluid density

τ = shear stress
τ_3 = shear rate measured at 3 rpm in a Fann viscometer
τ_6 = shear rate measured at 6 rpm in a Fann viscometer
τ_s = surplus stress
τ_w = wall shear stress
τ_y = yield stress

References

[1] Saasen, A., 2014, "Annular Frictional Pressure Losses During Drilling–Predicting the Effect of Drillstring Rotation," ASME J. Energy Resour. Technol., **136**(3), p. 034501.
[2] Sayindla, S., Lund, B., Ytrehus, J. D., and Saasen, A., 2017, "Hole-Cleaning Performance Comparison of Oil-Based and Water-Based Drilling Fluids," J. Pet. Sci. Eng., **158**, pp. 49–57.
[3] Werner, B., Myrseth, V., and Saasen, A., 2017, "Viscoelastic Properties of Drilling Fluids and Their Influence on Cuttings Transport," J. Pet. Sci. Eng., **156**, pp. 845–851.
[4] Bizhani, M., and Kuru, E., 2017, "Particle Removal From Sandbed Deposits in Horizontal Annuli Using Viscoelastic Fluids," SPE J., **23**, pp. 256–273.
[5] Li, J., and Luft, B., 2014, "Overview Solids Transport Study and Application in Oil-Gas Industry-Theoretical Work," International Petroleum Technology Conference, Kuala Lumpur, Malaysia, Dec. 10–12, Paper No. IPTC-17832-MS.
[6] Li, J., and Luft, B., 2014, "Overview of Solids Transport Studies and Applications in Oil and Gas Industry—Experimental Work," SPE Russian Oil and Gas Exploration & Production Technical Conference and Exhibition, Moscow, Russia, Oct. 14–16, Society of Petroleum Engineers, Paper No. SPE-171285-MS.
[7] Ytrehus, J. D., Lund, B., Taghipour, A., and Kosberg, B. R., 2021, "Hydraulic Behavior in Cased and Open Hole Sections in Highly Deviated Wellbores," ASME J. Energy Resour. Technol., **143**(3), p. 033008.
[8] Akhshik, S., Behzad, M., and Rajabi, M., 2016, "CFD-DEM Simulation of the Hole Cleaning Process in a Deviated Well Drilling: The Effects of Particle Shape," Particuology, **25**, pp. 72–82.
[9] Naganawa, S., Sato, R., and Ishikawa, M., 2017, "Cuttings-Transport Simulation Combined With Large-Scale-Flow-Loop Experimental Results and Logging-While-Drilling Data for Hole-Cleaning Evaluation in Directional Drilling," SPE Drill. Complet., **32**(3), pp. 194–207.
[10] Ytrehus, J. D., Lund, B., Taghipour, A., Kosberg, B. R., Carazza, L., Gyland, K. R., and Saasen, A., 2018, "Cuttings Bed Removal in Deviated Wells (OMAE2018-77832)," Proceedings of 37th International Conference on Ocean, Offshore and Arctic Engineering, June 17–22, ASME, Madrid.
[11] Saasen, A., and Ytrehus, J. D., 2018, "Rheological Properties of Drilling Fluids—Use of Dimensionless Shear Rates in Herschel-Bulkley Models and Power-Law Models," Appl. Rheol, **28**(5), p. 10.
[12] Saasen, A., and Ytrehus, J. D., 2020, "Viscosity Models for Drilling Fluids—Herschel-Bulkley Parameters and Their Use," Energies, **13**(20), p. 20.
[13] Power, D., and Zamora, M., 2003, "Drilling Fluid Yield Stress: Measurement Techniques for Improved Understanding of Critical Drilling Fluid Parameters (AADE-03-NTCE-35)," AADE 2003 National Technology Conference, Houston, TX, Apr. 1–3.
[14] Founargiotakis, K., Kelessidis, V. C., and Maglione, R., 2008, "Laminar, Transitional and Turbulent Flow of Herschel-Bulkley Fluids in Concentric Annulus," Can. J. Chem. Eng., **86**(4), pp. 676–683.
[15] Haciislamoglu, M., and Langlinais, J., 1990, "Non-Newtonian Flow in Eccentric Annuli," ASME J. Energy Resour. Technol., **112**(3), pp. 163–169.
[16] Haciislamoglu, M., and Cartalos, U., 1994, "Practical Pressure Loss Predictions in Realistic Annular Geometries," Paper No. SPE 28304, Proceedings of 69th SPE Annual Technical Conference and Exhibition, SPE, New Orleans, LA.
[17] Kelessidis, V. C., Dalamarinis, P., and Maglione, R., 2011, "Experimental Study and Predictions of Pressure Losses of Fluids Modeled as Herschel-Bulkley in Concentric and Eccentric Annuli in Laminar, Transitional and Turbulent Flows," J. Pet. Sci. Eng., **77**(3–4), pp. 305–312.
[18] Sterri, N., Saasen, A., Aas, B., and Hansen, S. A., 2000, "Frictional Pressure Losses During Drilling: Drill String Rotation Effects on Axial Flow of Shear Thinning Fluids in an Eccentric Annulus," Oil Gas Eur. Mag., **26**(3), pp. 30–33.